Archive of Applied Mechanics 70 (2000) 399–408 © Springer-Verlag 2000

Steady-state vibrations of an elastic beam on a visco-elastic layer under moving load

A. V. Metrikine, K. Popp

Summary The steady-state response of an elastic beam on a visco-elastic layer to a uniformly moving constant load is investigated. As a method of investigation the concept of "equivalent stiffness" of the layer is used. According to this concept, the layer is replaced by a 1D continuous foundation with a complex stiffness, which depends on the frequency and the wave number of the bending waves in the beam. This stiffness is analyzed as a function of the phase velocity of the waves. It is shown that the real part of the stiffness decreases severely as the phase velocity tends to a critical value, a value determined by the lowest dispersion branch of the layer. As the phase velocity exceeds the critical value, the imaginary part of the equivalent stiffness grows substantially. The dispersion relation for bending waves in the beam is studied to analyze the effect of the layer depth on the critical (resonance) velocity of the load. It is shown that the critical velocity is in the order of the Rayleigh wave velocity. The smaller the layer depth, the higher the critical velocity. The effect of viscosity in the layer on the resonance vibrations is studied. It is shown that the deeper the layer, the smaller this effect.

Key words Moving load, wave radiation, steady-state response, dispersion curves, critical velocity

1 Introduction

The velocity of modern high-speed trains can be in the order of the Rayleigh-wave velocity in the subsoil of a railroad track, especially if the trains move over soft soils, where the surface waves propagate with a velocity of 200–250 km/h. These waves, being radiated by the train, can strongly affect the dynamic behavior of the track. In developing a mathematical model of the track, this phenomenon has to be taken into account by including a 3D model of the subsoil. This was first done in [5], where the dynamic response of a beam on an elastic half-space to a moving constant load was considered. It was found that the load motion with the Rayleigh wave velocity causes resonance in the system. Later on, by means of the same model, it was shown in [8] that axial stresses in the beam reduce the critical velocity (this was first discovered in [6] in the frame work of a 1D model). Recently, the problem was reconsidered in [2] and it was found that there are two critical velocities of the load: one is equal to the Rayleigh wave velocity, and the other one is slightly smaller and equal to the minimum phase velocity of the waves in the beam.

Received 22 March 1999; accepted 26 July 1999

A. V. Metrikine (✉)
Delft University of Technology,
Faculty of Civil Engineering and Geosciences Stevinweg 1,
2628 CN Delft, The Netherlands
Tel.: 015 27844749; Fax: 015 2785767
E-mail: A.Metrikine@CT.TUDelft.nl

K. Popp
Faculty of Mechanical Engineering, Institute of Mechanics,
University of Hannover, Appelstrasse 11, D-30167 Hannover,
Germany
Tel.: +49 511 7624161; Fax: +49 511 7624164
E-mail: popp@ifm.uni-hannover.de

The paper contains results of investigations sponsored by the Alexander von Humboldt Foundation (Germany). This support is highly appreciated.

In all the above mentioned papers, the subsoil was modeled by a purely elastic half-space. It is evident, however, that the real subsoil possesses a viscosity and may be bounded. An attempt to consider the effect of viscosity was done in [1], where viscosity was included into model [5]. A solution was found for the problem, but no physical interpretation was given there. In [10], the subsoil was modeled as an elastic layer, taking into account a rigid boundary in the ground. There were considered, however, only the natural frequencies of the railroad track, paying no attention to its response to a moving load.

In this paper, we investigate vibrations of the beam on a visco-elastic layer under the action of a moving load. The goal of the study is to find the critical (resonance) velocities of the load, and to analyze the effect of the depth of the layer and its viscosity on the resonance vibrations.

The analysis is carried out using the "equivalent stiffness" concept, [2]. According to it, the layer is exactly replaced by an equivalent stiffness, continuously distributed along the beam. The equivalent stiffness is a complex function of the frequency and the wave number of waves in the beam. The dependence of the equivalent stiffness on the phase velocity of waves in the beam is carefully studied. This gives important preliminary information about the system response, since the phase velocity of waves excited by the load in the beam (in a steady state) is equal to the velocity of the load.

The dispersion relation for the bending waves in the beam is derived and analyzed. Using this relation and by means of a graphical analysis, see [3], the effect of the layer depth on the critical velocity of the load is determined.

Finally, by analyzing the beam is displacement under the load, the influence of the layer viscosity on the resonance vibrations is studied.

2
The model and governing equations

We consider a uniform $x = Vt$ motion of a constant load P along an Euler-Bernoulli beam on a visco-elastic layer of thickness H, as depicted in Fig. 1. The equations of motion of the layer can be written as, [7],

$$\tilde{\mu}\nabla^2\vec{U} + (\tilde{\lambda} + \tilde{\mu})\nabla\left(\nabla\vec{U}\right) = \rho\frac{\partial^2\vec{U}}{\partial t^2} \quad , \tag{1}$$

where $\vec{U}(x, y, z, t) = \{U_1, U_2, W\}$ is the vector of displacements, ρ is the mass density of the layer, $\tilde{\lambda} = \lambda + \lambda^*\partial/\partial t$ and $\tilde{\mu} = \mu + \mu^*\partial/\partial t$ are operators, which are used instead of Lamé's constants λ and μ to describe a visco-elastic behavior of the layer.

The layer is fixed at its bottom, the boundary conditions at $z = H$ read therefore

$$\vec{U}(x, y, H, t) = 0 \quad . \tag{2}$$

It is assumed that (a) the beam has a finite width $2a$, (b) both the load and the normal stresses σ_{zz} are uniformly distributed over the width of the beam, and (c) the contact between the beam and the layer is smooth, hence the shear stresses τ_{zx} and τ_{zy} are zero at the interface. Then, the balance of stresses at the surface of the layer can be written as

$$\begin{aligned} 2a\sigma_{zz}(x, y, 0, t) &= \left(m\frac{\partial^2 W^0}{\partial t^2} + EI\frac{\partial^4 W^0}{\partial x^4} + P\delta(x - Vt)\right)\Theta(a - |y|), \\ \tau_{zx}(x, y, 0, t) &= \tau_{zy}(x, y, 0, t) = 0 \quad , \end{aligned} \tag{3}$$

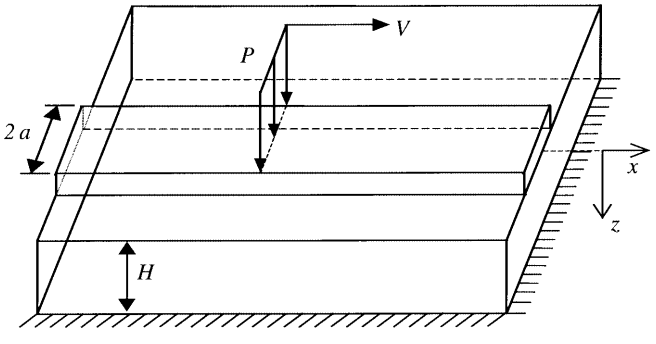

Fig. 1. Load motion along a beam on a 3D layer

where $W^0(x,t)$ is the vertical beam displacement, m and EI are the mass per unit length and the bending stiffness of the beam, $\Theta(\ldots)$ is the unit step function, $\delta(\ldots)$ is the Dirac delta-function.

Assuming that the centerline of the beam and the halfspace are always in contact, we write the compatibility condition as

$$W(x,0,0,t) = W^0(x,t) \ . \tag{4}$$

The equations of the layer motion (1) are satisfied by letting

$$U = \frac{\partial\varphi}{\partial x} + \frac{\partial^2\psi}{\partial x\partial z}, \quad V = \frac{\partial\varphi}{\partial y} + \frac{\partial^2\psi}{\partial y\partial z}, \quad W = \frac{\partial\varphi}{\partial z} + \frac{\partial^2\psi}{\partial z^2} - \nabla^2\psi \ , \tag{5}$$

provided that the two scalar functions $\varphi(x,y,z,t)$ and $\psi(x,y,z,t)$ are solutions of the following equations:

$$(\tilde{\lambda} + 2\tilde{\mu})\nabla^2\varphi = \rho\frac{\partial^2\varphi}{\partial t^2} \ , \quad \tilde{\mu}\nabla^2\psi = \rho\frac{\partial^2\psi}{\partial t^2} \ . \tag{6}$$

Expressions (5) and (6) are written in analogy to substitutions used by Lamb, [9], for a purely elastic solid. In terms of functions φ and ψ the stresses in the layer become

$$\begin{aligned} \tau_{xz} &= 2\tilde{\mu}\left(\frac{\partial^2\varphi}{\partial x\partial z} + \frac{\partial^3\psi}{\partial x\partial z^2}\right) - \rho\frac{\partial^3\psi}{\partial x\partial t^2}, \quad \tau_{yz} = 2\tilde{\mu}\left(\frac{\partial^2\varphi}{\partial y\partial z} + \frac{\partial^3\psi}{\partial y\partial z^2}\right) - \rho\frac{\partial^3\psi}{\partial y\partial t^2}, \\ \sigma_{zz} &= \tilde{\lambda}\nabla^2\varphi + 2\tilde{\mu}\left(\frac{\partial^2\varphi}{\partial z^2} + \frac{\partial^3\psi}{\partial z^3}\right) - 2\rho\frac{\partial^3\psi}{\partial z\partial t^2} \ . \end{aligned} \tag{7}$$

3
Equivalent stiffness of the layer

To analyze the problem, we will follow the concept of the "equivalent stiffness", [2]. According to this concept, firstly, an equivalent stiffness of the layer interacting with the beam has to be found. This allows an exact reduction of the initial 3D model to a one-dimensional model, namely to the load motion along the beam on a foundation with frequency- and wave number-dependent complex stiffness $\chi_{\mathrm{eq}}^{\mathrm{layer}}$, see Fig. 2.

To obtain an expression for the equivalent stiffness we apply the following Fourier transforms with respect to time and horizontal spatial coordinates:

$$\begin{aligned} f(k_1,k_2,z,\omega) &= \int_{-\infty}^{\infty}\int_{-\infty}^{\infty}\int_{-\infty}^{\infty}\varphi(x,y,z,\tau)\exp[i(\omega t - k_1x - k_2y)]\mathrm{d}t\,\mathrm{d}x\,\mathrm{d}y, \\ g(k_1,k_2,z,\omega) &= \int_{-\infty}^{\infty}\int_{-\infty}^{\infty}\int_{-\infty}^{\infty}\psi(x,y,z,\tau)\exp[i(\omega t - k_1x - k_2y)]\mathrm{d}t\,\mathrm{d}x\,\mathrm{d}y, \\ h(k_1,\omega) &= \int_{-\infty}^{\infty}\int_{-\infty}^{\infty}W^0(x,t)\exp(i\omega t - ik_1x)\mathrm{d}t\,\mathrm{d}x \ , \end{aligned} \tag{8}$$

where variables of integration ω, k_1 and k_2, respectively, represent the frequency and the wave numbers in the x- and y-directions of waves propagating in the system.

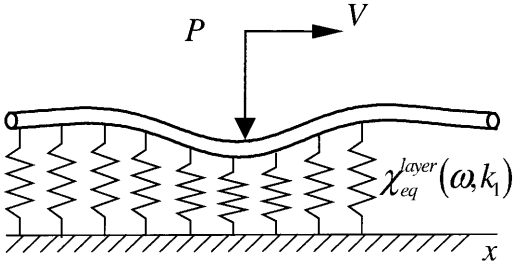

Fig. 2. Load motion along a 1D beam on an equivalent foundation

Application of Eq. (8) yields the following equations in the Fourier domain:

- For the layer motion, from Eq. (6),

$$\frac{\partial^2 f}{\partial z^2} + \left(\frac{\omega^2}{\tilde{c}_L^2} - k_1^2 - k_2^2\right) f = 0, \quad \frac{\partial^2 g}{\partial z^2} + \left(\frac{\omega^2}{\tilde{c}_T^2} - k_1^2 - k_2^2\right) g = 0 \ , \tag{9}$$

where

$$\tilde{c}_L^2 = c_L^2 - i\omega \frac{\lambda^* + 2\mu^*}{\rho}, \quad \tilde{c}_T^2 = c_T^2 - i\omega \frac{\mu^*}{\rho} \ ,$$

are complex values in which $c_L = \sqrt{(\lambda + 2\mu)/\rho}$ and $c_T = \sqrt{\mu/\rho}$ are the velocities of the dilatational and shear waves in the layer, respectively.

- For the displacements at the bottom $z = H$, from Eq. (2), using Eq. (5),

$$f + \frac{\partial g}{\partial z} = 0, \quad \frac{\partial f}{\partial z} + \frac{\partial^2 g}{\partial z^2} + \frac{\omega^2}{\tilde{c}_T^2} g = 0 \ . \tag{10}$$

- For the stress balance at the surface $z = 0$, from Eq. (3), using Eq. (7)

$$\begin{aligned} &2(\mu - i\omega\mu^*)\left(\frac{\partial f}{\partial z} + \frac{\partial^2 g}{\partial z^2}\right) + \rho\omega^2 g = 0, \\ &(\lambda - i\omega\lambda^*)\left(\frac{\partial^2 f}{\partial z^2} - k_1^2 - k_2^2\right) + 2(\mu - i\omega\mu^*)\left(\frac{\partial^2 f}{\partial z^2} + \frac{\partial^3 g}{\partial z^3}\right) + 2\rho\omega^2 \frac{\partial g}{\partial z} \\ &\quad = [h(\omega, k_1) D(\omega, k_1) + 2\pi P \delta(\omega - k_1 V)] \frac{\sin(ak_2)}{ak_2} \ , \end{aligned} \tag{11}$$

where

$$D(\omega, k_1) = -m\omega^2 + EIk_1^4$$

is the dispersion relation for the vertical vibrations of a free beam.

- For the compatibility condition, from Eq. (4)

$$h(\omega, k_1) = \frac{1}{2\pi} \int_{-\infty}^{\infty} w(k_1, k_2, 0, \omega) \mathrm{d}k_2 \ , \tag{12}$$

where

$$w(k_1, k_2, z, \omega) = \int_{-\infty}^{\infty} \int_{-\infty}^{\infty} \int_{-\infty}^{\infty} W(x, y, z, t) \exp(i(\omega t - k_1 x - k_2 y)) \mathrm{d}t \, \mathrm{d}x \, \mathrm{d}y$$

is the Fourier image of the layer vertical displacement.

The general solutions of Eqs. (9) are

$$\begin{aligned} f &= B_1 \sinh\left(z\tilde{R}_L\right) + B_2 \cosh\left(z\tilde{R}_L\right), \\ g &= B_3 \sinh\left(z\tilde{R}_T\right) + B_4 \cosh\left(z\tilde{R}_T\right) \ , \end{aligned} \tag{13}$$

where

$$\tilde{R}_{L,T} = \sqrt{k_1^2 + k_2^2 - \frac{\omega^2}{\tilde{c}_{L,T}^2}} \ .$$

Substituting Eq. (13) into boundary conditions (10), (11), and then solving the system of linear algebraic equations thus obtained with respect to B_j ($j = 1 \ldots 4$), one finds

$$B_j = \frac{\Delta_j}{\Delta} \quad , \tag{14}$$

where

$$\begin{aligned}
\Delta &= (\mu - i\omega\mu^*)^2\left[4K^2\gamma\tilde{R}_L\tilde{R}_T + K^2\left(4\tilde{R}_L^2\tilde{R}_T^2 + \gamma^2\right)\sinh(H\tilde{R}_L)\sinh(H\tilde{R}_T)\right.\\
&\qquad \left. -\tilde{R}_L\tilde{R}_T\left(4K^4 + \gamma^2\right)\cosh(H\tilde{R}_L)\cosh(H\tilde{R}_T)\right] \quad ,\\
\Delta_1 &= F\gamma(\mu - i\omega\mu^*)\left[\tilde{R}_L\tilde{R}_T\sinh(H\tilde{R}_L)\cosh(H\tilde{R}_T) - K^2\sinh(H\tilde{R}_T)\cosh(H\tilde{R}_L)\right] \quad ,\\
\Delta_2 &= F(\mu - i\omega\mu^*)\left[2K^2\tilde{R}_L\tilde{R}_T + \gamma K^2\sinh(H\tilde{R}_L)\sinh(H\tilde{R}_T) - \gamma\tilde{R}_L\tilde{R}_T\cosh(H\tilde{R}_L)\cosh(H\tilde{R}_T)\right] \quad ,\\
\Delta_3 &= F\tilde{R}_L(\mu - i\omega\mu^*)\left[\gamma + 2\tilde{R}_L\tilde{R}_T\sinh(H\tilde{R}_L)\sinh(H\tilde{R}_T) - 2K^2\cosh(H\tilde{R}_L)\cosh(H\tilde{R}_T)\right] \quad ,\\
\Delta_4 &= 2F\tilde{R}_L(\mu - i\omega\mu^*)\left[K^2\sinh(H\tilde{R}_T)\cosh(H\tilde{R}_L) - \tilde{R}_L\tilde{R}_T\sinh(H\tilde{R}_L)\cosh(H\tilde{R}_T)\right] \quad ,\\
K^2 &= k_1^2 + k_2^2, \quad \gamma = 2K^2 - \frac{\omega^2}{\tilde{c}_T^2}, \quad F = [h(\omega,k_1)D(\omega,k_1) + 2\pi P\delta(\omega - k_1V)]\frac{\sin(ak_2)}{ak_2} \quad .
\end{aligned}$$

To obtain an equation of motion for the beam in the Fourier domain one has to apply the compatibility condition. According to Eq. (5), the Fourier image of the vertical beam displacement reads

$$w(k_1,k_2,z,\omega) = \frac{\partial f}{\partial z} + \frac{\partial^2 g}{\partial z^2} - \left[\frac{\partial^2 g}{\partial z^2} - \left(k_1^2 + k_2^2\right)g\right] = \frac{\partial f}{\partial z} + \left(k_1^2 + k_2^2\right)g \quad .$$

Employing Eq. (14) and letting $z = 0$, one obtains

$$\begin{aligned}
w(k_1,k_2,0,\omega) &= \frac{F}{\Delta}\frac{\tilde{R}_L\omega^2}{\tilde{c}_T^2}(\mu - i\omega\mu^*)\\
&\quad \times\left[K^2\sinh(H\tilde{R}_T)\cosh(H\tilde{R}_L) - \tilde{R}_L\tilde{R}_T\sinh(H\tilde{R}_L)\cosh(H\tilde{R}_T)\right] \quad .
\end{aligned} \tag{15}$$

Substitution of Eq. (15) into the compatibility condition (12) gives finally the following equation of the beam motion in the Fourier domain:

$$h(\omega,k_1)[-m\omega^2 + EIk_1^4 + \chi_{\text{eq}}^{\text{layer}}(\omega,k_1)] = -2\pi P\delta(\omega - k_1V) \quad , \tag{16}$$

where

$$\chi_{\text{eq}}^{\text{layer}}(\omega,k_1) = -\frac{2\pi}{\omega^2}\tilde{c}_T^2(\mu - i\omega\mu^*)\left(\int_{-\infty}^{\infty}\tilde{R}_L\frac{\text{Num}(k_2)}{\text{Den}(k_2)}\frac{\sin(ak_2)}{ak_2}\,\mathrm{d}k_2\right)^{-1} \quad , \tag{17}$$

is the equivalent stiffness of the layer interacting with the beam and the following notation has been introduced:

$$\begin{aligned}
\text{Num}(k_2) &= K^2\sinh(H\tilde{R}_T)\cosh(H\tilde{R}_L) - \tilde{R}_L\tilde{R}_T\sinh(H\tilde{R}_L)\cosh(H\tilde{R}_T),\\
\text{Den}(k_2) &= 4K^2\gamma\tilde{R}_L\tilde{R}_T + K^2\left(4\tilde{R}_L^2\tilde{R}_T^2 + \gamma^2\right)\sinh(H\tilde{R}_L)\sinh(H\tilde{R}_T)\\
&\quad - \tilde{R}_L\tilde{R}_T\left(4K^4 + \gamma^2\right)\cosh(H\tilde{R}_L)\cosh(H\tilde{R}_T) \quad .
\end{aligned}$$

As one can see from Eq. (17), the equivalent stiffness of the layer is a function of the frequency ω and the wave number k_1 of the waves in the beam. To analyze $\chi_{\text{eq}}^{\text{layer}}(\omega,k_1)$, it is suitable, especially for the moving load problem, to introduce in Eq. (17) the following variable of integration and parameters: ratio $\xi = k_2/k_1$ of the wave numbers in the y and x directions; phase velocity $V_{\text{ph}} = \omega/k_1$ of the waves in the beam; the ratios $\beta_{L,T} = V_{\text{ph}}/\tilde{c}_{L,T}$; the dimensionless wave number $k = ak_1$ of the waves in the beam; the ratio $d = H/a$ of the layer depth and the half-width of the beam. In terms of these parameters, the equivalent stiffness reads

$$\chi_{\mathrm{eq}}^{\mathrm{layer}}\left(V_{\mathrm{ph}},k\right)=-2\pi\mu\left(1-ikV_{\mathrm{ph}}\frac{\mu^{*}}{\mu}\right)\left(\beta_T^2\int_{-\infty}^{\infty}R_L\frac{\mathrm{Num}(\xi)}{\mathrm{Den}(\xi)}\frac{\sin(k\xi)}{k\xi}\mathrm{d}\xi\right)^{-1}\quad,\tag{18}$$

where

$$\mathrm{Num}(\xi)=\left(1+\xi^2\right)\sinh(kdR_T)\cosh(kdR_L)-R_LR_T\sinh(kdR_L)\cosh(kdR_T)\quad,$$

$$\mathrm{Den}(\xi)=4\left(1+\xi^2\right)\gamma(\xi)R_LR_T+\left(1+\xi^2\right)4R_L^2R_T^2+\gamma(\xi)^2\sinh(kdR_L)\sinh(kdR_T)$$
$$-R_LR_T4\left(1+\xi^2\right)^4+\gamma(\xi)^2\cosh(kdR_L)\cosh(kdR_T),$$

$$R_{L,T}=\sqrt{1+\xi^2-\beta_{L,T}^2},\quad\gamma(\xi)=2+2\xi^2-\beta_T^2,\quad\beta_{L,T}=\frac{V_{\mathrm{ph}}}{\tilde{c}_{L,T}}=\frac{\omega}{k_1\tilde{c}_{L,T}}\quad.$$

To analyze the equivalent stiffness, one has to evaluate the integral in Eq. (18). It can be done either by the contour integration method or by direct numerical integration. The latter way seems to be more applicable here, since the integrand in (18) has no singularities due to the viscosity in the layer. So, we will proceed using the direct integration. Results of this integration are depicted in Fig. 3, where the equivalent stiffness is plotted as a function of the phase velocity V_{ph} for a constant wave number k. Calculations were carried out for the following parameters of the system: Poisson's ratio of the layer $\nu=0.3$; Lamé's constant of the layer $\mu=3.8*10^7\,\mathrm{N/m^2}$; the layer density $\rho=1.5*10^3\,\mathrm{kg/m^3}$; the viscosity parameters $\lambda^*=\mu^*=1.44*10^4\,\mathrm{Ns/m^2}$; the layer depth $H=9$ m; the beam width $2a=2.6$ m. Parameters of the layer are chosen to describe a realistic, though arbitrary, ground and the width of the beam represents the length of the sleepers.

The following conclusions can be drawn from Fig. 3:

1. The equivalent stiffness is a complex function. By definition, its real part reflects the elastic and the inertial properties of the equivalent foundation, while the imaginary part is related to the energy dissipation in the foundation.
2. The imaginary part of the equivalent stiffness becomes significant when the phase velocity exceeds the critical value V_{ph}^{*}, which is indicated in Fig. 3. This critical value depends on the wave number k as shown in Fig. 4. This dependence represents the phase velocity variation in the lowest dispersion branch of the elastic layer, see [4]. The reason for the imaginary part of $\chi_{\mathrm{eq}}^{\mathrm{layer}}$ to significantly grow for $V_{\mathrm{ph}}>V_{\mathrm{ph}}^{*}$ is the radiation into the layer. These waves, extracting energy from the beam, provide substantial equivalent attenuation of waves in the beam.
3. Both the real and the imaginary part of the equivalent stiffness have a set of minima for $V_{\mathrm{ph}}>V_{\mathrm{ph}}^{*}$. These minima arise when, for a given value of the wave number k, V_{ph} is close to the group velocity of one of the higher modes of the layer vibrations. If the layer had no viscosity, the equivalent stiffness in these points would be zero.
4. When the phase velocity tends to V_{ph}^{*}, the equivalent stiffness becomes rather small (both the real and the imaginary part). One has to keep this in mind, since the decrease of the equivalent stiffness is, in fact, the basic reason for resonance in a system subjected to a moving load, see, e.g., [2].

Thus, waves with phase velocities smaller than V_{ph}^{*} can propagate in the beam with almost constant amplitude (losses are quite small since the imaginary part of the equivalent stiffness

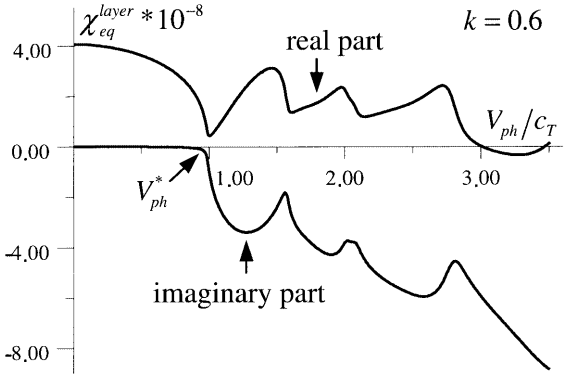

Fig. 3. Equivalent stiffness of the layer as a function of phase velocity of waves in the beam

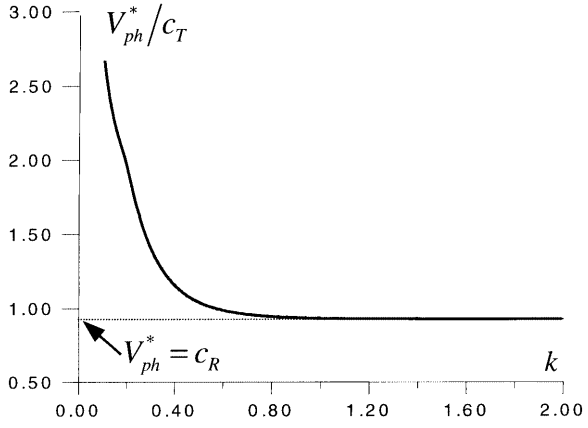

Fig. 4. Relative phase velocity V^*_{ph}/c_T versus wave number k for the lowest dispersion branch of the layer

is small). This fact gives us an idea that critical velocities of the load can occur related to what is known as the "wave resonance", see [3, 11]. This resonance arises when the velocity of a load is equal to the group velocity of waves radiated by the load.

These velocities will be investigated in the next section by analyzing the beam dispersion.

4
Dispersion curve of the beam and critical velocities of the load

To analyze the wave propagation in the beam, we will temporarily suppose that the viscosity in the layer is zero. In this case waves can propagate in the beam with constant amplitude. However, even in the absence of viscosity, not all waves in the beam (with an arbitrary frequency and wave number) will be undamped, but only those that excite no waves in the layer. As discussed in the previous section, such waves should have phase velocities smaller than V^*_{ph} (the phase velocity of the lowest mode of the layer). Therefore, in order to find propagating waves in the beam, we will analyze the dispersion equation of the layer, see Eq. (16),

$$-m\omega^2 + EIk_1^4 + \chi_{\mathrm{eq}}^{\mathrm{layer}}(\omega, k_1) = 0 \ , \tag{19}$$

in the range $V_{\mathrm{ph}} < V^*_{\mathrm{ph}}$. In this range, the equivalent stiffness can be calculated by direct integration, since the integrand in Eq. (18) has no singularities even for vanishing viscosity in the layer. Results of the numerical evaluation of Eq. (18) are depicted in Fig. 5a, b. In these figures the dispersion curves of the beam are plotted for two different depths of the layer. The curves represent real pairs $\{\omega, k_1\}$, which are solutions of Eq. (19). The parameters of the layer are taken as in the previous section (only $\lambda^* = \mu^* = 0$), and the parameters of the beam are as follows: the beam mass per unit length $m = 1700$ kg/m (we included the mass of the rails, sleepers and ballast); the beam flexural rigidity $EI = 1.3 * 10^8\,\mathrm{Nm}^2$, the beam width $2a = 3$ m.

The dispersion curves in the figures are denoted bold. The dashed lines represent the lowest dispersion branch of the layer. The straight line shows the phase velocity equal to the Rayleigh wave velocity in the layer as $H \to \infty$ (the dispersion branches of the layer tend to this line, as k_1 grows). The figures show the following:

1. The dispersion curves of the beam (note that these curves show only waves propagating without energy losses) exist only in intervals of relatively small wave numbers. The curves disappear as they cross the lowest dispersion branch of the layer, since beam vibrations begin generating waves in the layer.
2. The dispersion curves of the beam are close to the lowest dispersion curve of the layer. This shows that the effect of the beam itself on the dispersion properties of the whole system is relatively small (even in the case plotted in the figures, where the beam represents the rails, the sleepers and the ballast). The larger the layer depth, the closer the beam dispersion curve to the lowest branch of the layer.

It is of particular importance that Fig. 5 allows determination of the critical (resonance) velocity of a constant load moving along the beam with a constant velocity. Under the

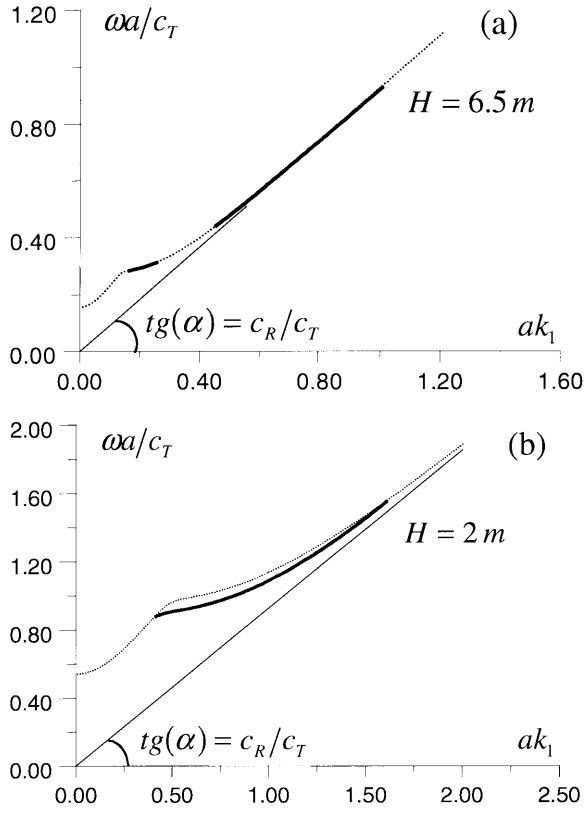

Fig. 5. Dispersion curves (bold) for vertical bending waves in the beam

motion with such a velocity, the steady-state beam displacement becomes infinite in the absence of viscosity. The viscosity limits the value of the resonance displacement. The critical velocity can be determined from Fig. 5 in the following way: one has to find the slope of a straight line, which, crossing the origin, is tangential to the dispersion curve of the beam (see [3, 11]). The slope of this line equals to the ratio of the critical velocity and the shear wave velocity c_T. The physical significance of this graphical determination is quite simple: if the line is tangent to the dispersion curve, then the velocity of the load is equal to the group velocity of a wave radiated by the load. Therefore, the energy radiated by the load moves with the load and increases in time, since the radiation is a continuous process. Evidently, this process will lead to an infinite growth of the beam displacement. Of course, if there is viscosity in the layer, other damping mechanisms or some nonlinearities, the resonance will be limited or even avoided.

As one can see from Fig. 5, the critical velocity of the load is close to the Rayleigh wave velocity c_R. However, as the layer depth decreases, the critical velocity slightly increases. This qualitative conclusion will be verified in the next section, where the beam displacement will be calculated and the effect of viscosity on the beam vibrations will be analyzed.

5
Steady-state response of the beam to the load

To determine the steady-state beam displacement caused by the moving load, one has to apply to Eq. (16) the inverse Fourier transforms with respect to frequency ω and wave number k_1, which yields

$$\begin{aligned} W^0(x,t) &= \frac{1}{4\pi^2}\int_{-\infty}^{\infty}\int_{-\infty}^{\infty} h(\omega,k_1)\exp(ik_1x - i\omega t)\mathrm{d}\omega\,\mathrm{d}k_1 \\ &= -\frac{P}{2\pi}\int_{-\infty}^{\infty}\int_{-\infty}^{\infty}\frac{\delta(\omega - k_1V)\exp(ik_1x - i\omega t)}{-m\omega^2 + EIk_1^4 + \chi_{\mathrm{eq}}^{\mathrm{layer}}(\omega,k_1)}\mathrm{d}\omega\,\mathrm{d}k_1 \\ &= -\frac{P}{2\pi}\int_{-\infty}^{\infty}\frac{\exp[ik_1(x - Vt)]}{-mk_1^2V^2 + EIk_1^4 + \chi_{\mathrm{eq}}^{\mathrm{layer}}(k_1V,k_1)}\mathrm{d}k_1\ . \end{aligned} \tag{20}$$

Using the following symmetry properties of $\chi_{eq}^{layer}(k_1 V, k_1)$:

$$\mathrm{Re}\left[\chi_{eq}^{layer}(k_1 V, k_1)\right] = \mathrm{Re}\left[\chi_{eq}^{layer}(-k_1 V, -k_1)\right];$$
$$\mathrm{Im}\left[\chi_{eq}^{layer}(k_1 V, k_1)\right] = -\mathrm{Im}\left[\chi_{eq}^{layer}(-k_1 V, -k_1)\right] \ ,$$

one can rewrite Eq. (20) in the form

$$W^0(x,t) = -\frac{P}{\pi}\int_0^\infty \frac{A_1(k_1)\cos[k_1(x-Vt)] + A_2(k_1)\sin[k_1(x-Vt)]}{\left\{-mk_1^2V^2 + EIk_1^4 + \mathrm{Re}\left[\chi_{eq}^{layer}(k_1 V, k_1)\right]\right\}^2 + \mathrm{Im}\left[\chi_{eq}^{layer}(k_1 V, k_1)\right]^2}\,\mathrm{d}k_1 \ , \tag{21}$$

where

$$A_1(k_1) = -mk_1^2V^2 + EIk_1^4 + \mathrm{Re}\left[\chi_{eq}^{layer}(k_1 V, k_1)\right], \qquad A_2(k_1) = \mathrm{Im}\left[\chi_{eq}^{layer}(k_1 V, k_1)\right] \ .$$

The integrand in Eq. (21) tends to zero proportionally to $1/k_1^4$ (i.e. fast) as $k_1 \to \infty$, and has no singularities on the integration path. Therefore, it is not a problem to calculate the integral in Eq. (21) numerically. The corresponding results are depicted in Fig. 6, where the beam displacement under the load ($x = Vt$) is plotted as a function of the load velocity. The displacement is depicted for different depths of the layer. The other parameters of the system are taken as in the previous section ($\nu = 0.3$; $\mu = 3.8 * 10^7\,\mathrm{N/m^2}$; $\rho = 1.5 * 10^3\,\mathrm{kg/m^3}$; $m = 1700\,\mathrm{kg/m}$; $EI = 1.3 * 10^8\,\mathrm{Nm^2}$; $2a = 2.6\,\mathrm{m}$); additionally, the viscosity parameters of the layer are $\lambda^* = \mu^* = 1.44 * 10^4\,\mathrm{Ns/m^2}$.

One can see from Fig. 6 that, according to results of the previous section, the resonance velocity of the load, which gives a maximum amplification in the displacement, decreases slightly as the depth of the layer increases. The dependences are rather different if the depth is relatively small (compare the curves for $H = 1.7\,\mathrm{m}$ and $H = 4.7\,\mathrm{m}$). For larger depths, the curves are almost the same, and only near the resonance velocity a small difference can be seen.

The most important result reflected by Fig. 6 is that the resonance amplification is substantially smaller when the depth of the layer is smaller. This brings the following idea, which can be interesting for practical applications. To make the dynamical amplification of the track vibrations at the critical train velocities smaller, one can put a stiff strip under the track, providing an artificial boundary. This boundary will slightly increase the critical velocity of the train and make the influence of the viscosity in the subsoil more effective. Such a stiff strip can be especially useful for soft subsoil where the critical velocity of the train is quite small since the Rayleigh wave velocity is in the range of 200–250 km/h.

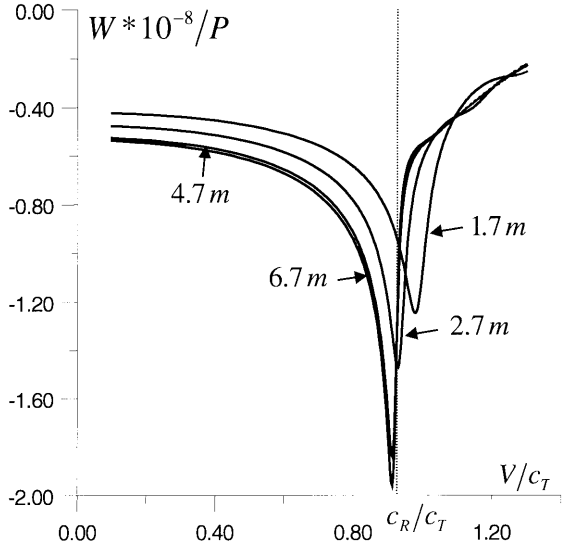

Fig. 6. Displacement under the load versus velocity of motion

6 Conclusions

In this paper, the steady-state vibrations of an elastic beam on a visco-elastic layer under a uniformly moving constant load have been investigated. First, the 3D layer has been exactly replaced by a 1D equivalent foundation, continuously distributed along the beam. It was shown that the equivalent stiffness of this foundation is a complex function dependent on the frequency of the beam vibrations and the wave number of waves in the beam. The real part of the equivalent stiffness reflects elasto-inertial properties of the layer, and the imaginary part is responsible for the attenuation of the beam vibrations. This attenuation can happen due to the viscosity in the layer and as a result of the radiation of waves into the layer. Analyzing the equivalent stiffness, it was found that its imaginary part becomes substantially larger when the phase velocity of waves in the beam exceeds a critical value V^*_{ph}. This critical phase velocity is determined by the lowest dispersion branch of the layer, and the increase of the imaginary part is related to the wave radiation in the layer caused by the beam vibrations. Since the layer is a dispersive system, V^*_{ph} is a function of the wave number of waves propagating along the beam. The real part of the equivalent stiffness dramatically decreases, as the phase velocity of waves in the beam approaches V^*_{ph}.

In the range $V_{\mathrm{ph}} < V^*_{\mathrm{ph}}$ of the phase velocities, waves in the beam can propagate with almost constant amplitudes, slightly attenuated only by the viscosity in the layer. Therefore, the analysis of the dispersion properties of the beam has a physical significance in this range. It was shown that the dispersion curve of the beam is located close to the lowest dispersion branch of the layer, and exists only for relatively long waves in the beam. The deeper the layer, the closer this dispersion curve to that given by the lowest branch of the layer.

The steady-state beam displacement under the moving load has been investigated. It has been shown that there exists a critical (resonance) velocity of the load, which gives a substantial dynamical amplification of the beam vibrations. This critical velocity is close to the Rayleigh wave velocity in the layer. As the depth of the layer grows, the critical velocity becomes slightly smaller. On the other hand, the effect of viscosity in the layer on the resonance vibrations of the beam increases as the layer depth decreases.

References

1. **Bogacz, R.:** On dynamics and stability of continuous systems subjected to a distributed moving load. Archives of Mechanics 53 (1983) 243–255
2. **Dieterman, H. A.; Metrikine, A. V.:** The equivalent stiffness of a half-space interacting with a beam. Critical velocities of a moving load along the beam. Eur. J. Mech. S/A 15/1 (1996) 67–90
3. **Dieterman, H. A.; Metrikine, A. V.:** Critical velocities of a harmonic load moving uniformly along an elastic layer. J. Appl. Mech. ASME 64 (1997) 596–600
4. **Ewing, W. M.; Jardetsky, W. S.; Press F.:** Elastic Waves in Layered Media. New York: McGraw-Hill 1957
5. **Filippov, A. P.:** Steady state vibrations of an infinite beam on an elastic half-space subjected to a moving load. Izvestija AN SSSR OTN Mechanika I Mashinostroenie 6 (1961) 97–105
6. **Kerr, A. D.:** The continuously supported rail subjected to an axial force and a moving load. Int. J. Mech. Sci. 14 (1972) 71–78
7. **Kolsky, H.:** Stress waves in solids. Oxford: Clarendon Press 1953
8. **Labra, J. J.:** An axially stressed railroad track on an elastic continuum subjected to a moving load. Acta Mech. 22 (1975) 113–129
9. **Lamb, H.:** On the propagation of tremors over the surface of an elastic solid. Phil. Trans. Roy. Soc. London A203/1 (1904) 1–42
10. **Patil, S. P.:** Natural frequencies of a railroad track. J. Appl. Mech. ASME 54 (1987) 299–304
11. **Vesnitskii, A. I.:** Wave effects in elastic systems. In: Frolow, K. V. (ed.) Wave dynamics of Machines, pp. 15–30. Moscow: Nauka 1991 (in Russian)